Design, Synthesis, Radiolabeling and *In Vitro* and *In Vivo* Characterization of Tumor-antigen- and Antibody-derived Peptides for the Detection of Breast Cancer

SUBHANI M. OKARVI and IBRAHIM A. JAMMAZ

Cyclotron and Radiopharmaceuticals Department,
King Faisal Specialist Hospital and Research Centre, Riyadh, Saudi Arabia

Abstract. *HER2/neu and MUC1-based synthetic peptides were prepared and evaluated in an effort to develop peptide-based radiopharmaceuticals derived from tumor-associated-antigens for the detection of breast cancer. The receptors for HER2/neu and MUC1 are overexpressed in various human cancers, such as breast and ovarian cancer. The relatively low expression of these antigens on normal tissues makes them attractive targets for tumor imaging. In addition, antitumor-antibody-derived peptides based on the Glu-Pro-Pro-Thr (EPPT) sequence were prepared for the detection of breast cancer. It has been shown that the EPPT peptide has high affinity for the MUC1-derived peptide. The peptides were prepared by solid-phase synthesis and radiolabeled efficiently with ^{99m}Tc via ligand exchange. They exhibited good stability in vitro in human plasma and against cysteine and histidine challenge. The peptides displayed high affinities (in nanomolar range) for MCF-7, MDA-MB-231 and T47-D breast cancer cell lines in vitro. Additionally, they exhibited a rapid internalization into tumor cells. In vivo biodistribution in mice showed rapid and efficient blood clearance and excretion mainly through the renal-urinary route, with some elimination via the hepatobiliary pathway. However, the extent of urinary excretion was found to be variable for radiopeptides, with the highest being observed for antitumor-antibody-derived peptide. The peptides showed moderate tumor uptake (up to 2.2±0.98% ID/g) in nude mice carrying breast tumor xenografts. The uptake in the tumor was always higher than in the blood and muscle. A fast clearance from the blood and low accumulation (<6% ID/g) by the major organs was obtained in nude mice resulting in favorable tumor/blood and tumor/muscle ratios as early as 1 h after injection. The combination of favorable in vitro and in vivo characteristics makes this new and interesting class of peptides potential candidates for the diagnosis of breast cancer in vivo.*

Correspondence to: S.M. Okarvi, Cyclotron and Radiopharmaceuticals Department, King Faisal Specialist Hospital and Research Centre, MBC-03, PO Box 3354, Riyadh 11211, Saudi Arabia. Tel: +96 614424812, Fax: +96 614424743, e-mail: sokarvi@kfshrc.edu.sa

Key Words: Breast cancer, tumor-antigen peptides, radiolabeling, tumor-cell binding, biodistribution.

Many tumor-associated antigens (TAAs) have been discovered and identified in the last decade and have provided new hope for the treatment of patients with malignant disease (1, 2). For the potential treatment of breast and ovarian cancer, however, only a few T-cell epitopes have been identified, including those derived from the *HER2/neu* proto-oncogene and the epithelial mucin, *MUC1* (1-3). Most tumor antigens are not only expressed in cancer cells but also in normal cells. One problem with this is that if tumor immunity is focused on antigens which are also expressed in normal cells (*i.e.* autoantigens), then any effect on tumor cells may cause an autoimmune response (4). Some tumor-specific antigens are derived from proteins that are structurally abnormal or completely silent in normal tissues. The human epithelial mucin encoded by the gene *MUC1* is an example of a tumor-specific antigen that is silent on normal tissues but it is overexpressed on almost all human epithelial cell cancers, including >90% of human breast, ovarian, pancreatic, colorectal, lung, prostate and gastric cancers (2, 5), thus making MUC1 a promising tumor-antigen with diagnostic as well as therapeutic potential in the management and treatment of cancer (5, 6). Another TAA that is amplified and/or overexpressed in several human cancers including breast and ovarian cancer is HER2 (human epidermal growth factor receptor type 2) also called HER2/neu, the gene product of *c-erbB-2* proto-oncogene (1, 3). Gene amplification and overexpression of HER2/neu have been demonstrated with high frequency in a number of human malignancies including breast and ovarian tumors (7). The overexpression of HER2/neu in various tumor cells and relatively low expression of this antigen in normal tissues (8-11), may make it an attractive target for tumor imaging with suitably designed HER2/neu-derived synthetic peptides. The

frequency of HER2/neu overexpression in various cancers and its importance in mediating cancer cell growth and aggressiveness have resulted in the development of a humanized monoclonal antibody, trastuzumab (Herceptin™). Blocking of HER2/neu signaling in breast cancers using the anti-HER2/neu antibody trastuzumab results in growth inhibition of tumor cells and an increase in the patients' survival rate (7, 11). Herceptin™ has been approved for clinical use in the U.S.A. and in Europe for the treatment of metastatic breast cancer (11, 12).

Scintigraphic detection of HER2/neu-positive breast cancer may provide important diagnostic information influencing patient management. The use of radionuclide diagnostic imaging would enable detection of HER2/neu expression by a non-invasive procedure in both primary tumors and metastases, without false-negative results due to biopsy sampling errors (11). Clinical utility of radionuclide imaging of HER2/neu expression in breast cancer patients has been demonstrated recently by using ^{111}In-DTPA-trastuzumab (13-15). Moreover, radionuclide targeting of HER2/neu, for both imaging and therapy, using intact antibodies has already been evaluated (11, 15-20). However, slow tumor targeting and slow blood clearance of intact antibodies are the well-known problems, and the use of small targeting agents seems to be crucial in future nuclear medicine, at least for diagnostic imaging (11, 21). The use of synthetic peptides in cancer diagnosis offers practical advantages over antibodies, such as relative ease of construction and production, chemical stability and a lack of infectious or oncogenic potential (10, 22, 23). It was assumed that synthetic peptides derived from TAAs and retaining most of the original affinity and specificity to tumor-antigens would be more suitable for tumor imaging. Though no information is available about the presence of specific receptor and/or binding affinity for the tumor-antigen-derived peptides HER2/neu and MUC1, there was an interest to determine whether these tumor-antigen-derived peptides have the ability to bind to breast cancer cells that express receptors for these peptides. In an effort to develop peptides derived from TAAs for imaging breast cancer, novel HER2/neu and MUC1-derived peptides were synthesized together with antitumor-antibody derived EPPT peptides and were coupled with MAG_3 (mercaptoacetyltriglycine) chelator for radiolabeling with technetium-99m (^{99m}Tc). ^{99m}Tc is the radionuclide of choice in the development of imaging agents by virtue of its wide availability (from ^{99m}Tc-generator system), short half-life (6 h), and ideal energy (140 keV) for γ-imaging (23). MAG_3 chelating moiety is used because of its feasibility of coupling to the targeting peptide molecules during peptide synthesis and its well-defined chemistry (24). The synthesized peptides include: HER2/neu-derived peptide (MAG_3-HER2/neu, MAG_3-(D)Asp^1-Lys^2-Ile^3-(D)Phe^4-Gly^5-Ser^6-Leu^7-Ala^8-(D)Phe^9-Leu^{10}-$CONH_2$) (3, 25-27), and the peptide derived from the breast cancer-associated mucin, MUC1 (MAG_3-MUC1, MAG_3-(D)Asp^1-Pro^2-(D)Asp^3-Thr^4-Arg^5-Pro^6-$CONH_2$) (5, 28). Moreover, a hybrid peptide, which combines the important amino acid sequences of two distinct TAAs, HER2/neu and MUC1 (MAG_3-HER2/neu-MUC1, MAG_3-(D)Asp^1-Lys^2-Ile^3-(D)Phe^4-Gly^5-Ser^6-Leu^7-Ala^8-(D)Phe^9-Leu^{10}-Pro^{11}-(D)Asp^{12}-Thr^{13}-Arg^{14}-Pro^{15}-$CONH_2$) was synthesized. In addition, a small peptide was prepared (MAG_3-EPPT, MAG_3-(D)Asp^1-Glu^2-Pro^3-Pro^4-Thr^5-$CONH_2$), derived from the CDR3 V_H region of a tumor-associated monoclonal antibody (ASM2), raised against human epithelial cancer cells. The immunological affinity of this peptide is mainly based on the EPPT residues in its sequence (5, 29, 30). It has been shown that the synthetic EPPT peptide has significant affinity for the MUC1-derived peptides (5). A hybrid peptide containing the critical amino acid sequences of both EPPT and MUC1 was also synthesized (MAG_3-EPPT-MUC1, MAG_3-(D)Asp^1-Glu^2-Pro^3-Pro^4-Thr^5-Pro^6-(D)Asp^7-Thr^8-Arg^9-Pro^{10}-$CONH_2$), and its potential as a tumor imaging agent was explored. In a previous study, the full length EPPT peptide was evaluated for the detection of breast cancer *in vivo* (29).

Herein, the continued research on the development of new peptide-based radiopharmaceuticals for tumor imaging, the synthesis, radiolabeling with ^{99m}Tc, and *in vitro* and *in vivo* characterization of a new and interesting class of radiopharmaceuticals derived from the TAAs and antitumor-antibody for the detection of breast cancer are described.

Materials and Methods

Preparation of peptides. All peptides were prepared by solid-phase synthetic techniques on a CS036 peptide synthesizer (CS Bio Co., San Carlos, CA, USA), following standard Fmoc (9-fluorenylmethoxycarbonyl) chemistry (31), using Rink amide MBHA (4-methylbenzhydrylamine) resin according to a general method described previously (29). Briefly, after stepwise incorporation of all the desired amino acids to the sequence, the last *N*-terminal Fmoc-protecting group was removed and *S*-benzoylmercaptoacetic acid (synthesized by reacting mercaptoacetic acid with benzoic acid chloride in the presence of a base) (32), was manually coupled to the free *N*-terminus of each peptide to yield MAG_3-peptide conjugates. The purity of each peptide was confirmed by HPLC and their identity by mass spectrometry.

Radiolabeling with ^{99m}Tc. A volume of 25-50 μL of each peptide (1 mg/mL CH_3CN/H_2O solution) was mixed with 200 μL 0.5 M citrate-phosphate buffer (pH 9-11), 250 μL (10 mg) sodium potassium tartrate solution and 20 μL 5% ascorbic acid. To this, 100 μL (100 μg) of $SnCl_2.2H_2O$ in 0.05 N HCl were added followed by 100-300 μL of $^{99m}TcO_4^-$ (5-15 mCi). The labeling mixture was then heated at 90°C for 10 min. The final pH of the reaction mixtures was between 7 and 9.

HPLC purification and analysis. HPLC analysis and purification of all five peptides and their metal complexes were performed on a Shimadzu HPLC system (Shimadzu Corporation, Kyoto, Japan) using a C_{18} reversed-phase column (5 μm, 3.9×150 mm) (DeltaPak, Waters Corporation, Milford, MA, USA). HPLC was run using a gradient system of 0.1% (v/v) TFA in water and 0.1% (v/v) TFA in acetonitrile at a flow rate of 0.9 mL/min. For each peptide, the major peak was isolated and the solvent was evaporated. The HPLC-purified compounds were reconstituted in sterile saline and used for cell-binding and animal biodistribution studies.

Cysteine and histidine challenge. The bond strength of ^{99m}Tc-complexes was determined by displacement of peptide bound radioactivity with cysteine and histidine. A known amount of each radiopeptide was incubated with an excess amount of cysteine or histidine (100-fold molar excess compared to the peptide) at 37˚C for up to 4 h. For transchelation studies, peptides were not purified by HPLC after labeling, hence, some tin, $^{99m}TcO_4^-$ or unlabeled peptides remained present in the solutions. The samples were analyzed at 1 and 4 h after incubation by HPLC and the percentage radioactivity associated with the cysteine or histidine and the intact radiolabeled peptides were determined.

Octanol–saline partition coefficient. To determine the lipophilicity, HPLC-purified radiopeptides (100 μL, ~100 μCi) were added to separate test tubes each containing 1 mL of *n*-octanol and 1 mL of saline. The tubes were vortexed for 1 min. After partial separation of the phases by gravity for another 15 min, 0.5 mL of each phase was transferred to separate tubes and centrifuged. Duplicate 100 μL aliquots of each phase were measured and the partition coefficient was determined by the function:
Partition coefficient=Log_{10} (radioactivity in octanol layer/radioactivity in aqueous layer) (33).

In vitro stability in plasma and in T47-D cells. Each radiopeptide (100 μL, ~500 μCi) was incubated with human plasma (500 μL) in duplicate at 37˚C for up to 4 h. Following incubation at 1 and 4 h, the plasma proteins were precipitated with a mixture of acetonitrile/ethanol (1:1 v/v) and the sample was centrifuged. The supernatant layer was filtered through a 0.2-μm pore filter and analyzed by HPLC. The stability in the cell culture was examined by incubating each ^{99m}Tc-peptide (50 μL, 100 μCi) with T47-D cells suspension (~200,000 cells in 200 μL) in phosphate-buffered saline (PBS) at 37˚C for 1 h. The mixtures were then centrifuged and the supernatant layers were analyzed by HPLC.

In vitro cell-binding and internalization. The cell-binding and subsequent internalization into MCF-7, MDA-MB-231 and T47-D breast cancer cell lines (American Type Culture Collection, Rockville, MD, USA) of peptides were performed according to the method described previously with a few modifications (34). In brief, approximately 300,000 cells (in 300 μL PBS) were incubated with various amounts of peptides (prepared from the serial dilutions of HPLC-purified radiopeptides) in duplicate for 1 h at room temperature. Incubation was terminated by dilution with cold saline (300 μL) and the cells were pelleted by centrifugation. The cell-pellets were rapidly washed with cold saline to remove any unbound peptide and centrifuged to collect supernatants. Radioactivity in the cell-pellet and the washings was measured in a γ-counter. Non-specific binding was determined in the presence of approximately 100-fold excess of unlabeled peptide. Specific binding was calculated by subtracting the non-specifically bound radioactivity from that of the total binding. The data were analyzed (to estimate respective binding affinities) by a non-linear regression analysis program (Phillip H. Sherrod, Brentwood, TN, USA) using one-site binding equation (35). Thereafter, the cell pellets were incubated again with 300 μL of acidic buffer (0.02 M sodium acetate in saline, pH 5.0) (36) at 37˚C for 20 min to allow cellular internalization of the surface bound radioligand (34, 37). After incubation, cells were separated by centrifugation. The amount of cell surface-bound (acid-wash) and intracellular radioactivity (acid-resistant) was determined by measuring the radioactivity of the supernatants and the cell-pellets, respectively, in a γ-counter (34).

In vivo animal biodistribution. Prior approval was obtained from the institutional Animal Safety and Care Committee for the use of animals. Animal studies were conducted according to the international regulations governing the safe and proper use of laboratory animals (38). *In vivo* biodistribution studies were performed on healthy Balb/c mice (body mass 18-25 g) and nude mice implanted with MDA-MB-231 cells. The HPLC-purified radioligands (100 μL, ~10 μCi, total peptide dose ≤1 μg) were injected intravenously *via* the lateral tail vein and the animals (n=3 animals per time point) were sacrificed by neck dislocation at 1 and 4 h post-injection (*p.i.*). The blood and urine were immediately collected. Any urine expelled on sacrificing the animals was measured together with that remaining in the bladder. Major organs (lungs, stomach, liver, kidneys and intestines) were excised, weighed and their radioactivity measured in a γ-counter. The percentage injected dose per gram (% ID/g) of tissue was calculated by counting the samples in a γ-counter against the suitably diluted aliquots of the injected solution as a standard. For clearance studies, radioactivity in the urine with bladder and intestines with contents is reported as the percentage of the injected dose (% ID). For the induction of tumor xenografts, estrogen-independent and highly aggressive MDA-MB-231 cells were subcutaneously injected at a concentration of 1×10^7 cells per mouse and allowed to grow *in vivo* for 3-4 weeks. After adequate growth of the tumors (0.6-1.0 g), tumor uptake studies were performed and the amount of radioactivity in the tumor and other major organs was determined by γ-counting as stated above for Balb/c mice.

Results and Discussion

Tumor targeting with small radiolabeled receptor-binding peptides is an attractive approach for the diagnosis and therapy of cancer (23). Many human tumors overexpress a variety of receptors for various peptides, which is the basis of peptide receptor-targeted imaging in nuclear medicine. The rapid pharmacokinetics and high affinity of radiopeptides for receptors on tumor cells can be effectively used for diagnosis and peptidic radionuclide therapy (23). Receptors for tumor-antigens, such as HER2/neu and MUC1, are commonly found preferentially on various tumor cells than in normal cells (4, 10, 11, 16), providing the basis for successful use of tumor-antigen-derived peptides for tumor imaging. One attractive way for developing compounds for targeting HER2/neu- and MUC1-positive tumors is the use

Table I. *Analytical data for the compounds synthesized in this study.*

Compound	Molecular formula	Calculated molecular weight	Experimental molecular weight $[M + H]^+$	HPLC t_R (min)
MAG_3-HER2/neu	$C_{69}H_{99}N_{15}O_{18}S_1$	1458	1459	20.0
MAG_3-MUC1	$C_{43}H_{61}N_{13}O_{16}S_1$	1047	1048	14.2
MAG_3-HER2/neu-MUC1	$C_{93}H_{137}N_{23}O_{26}S_1$	2024	2025	18.6
MAG_3-EPPT	$C_{38}H_{51}N_9O_{15}S_1$	905	906	14.0
MAG_3-EPPT-MUC1	$C_{62}H_{89}N_{17}O_{23}S_1$	1472	1473	14.3

of peptides derived from these tumor-specific antigens. An advantage of such peptide molecules is that they can be easily synthesized chemically and modified molecularly according to pharmacokinetic requirements. In this study, biologically active minimal sequences of human-tumor-derived peptides were designed for easy preparation and handling in order to evaluate their potential as breast cancer imaging agents.

Preparation of peptides. All peptides investigated in this study were conveniently and successfully prepared by solid-phase peptide synthesis using standard Fmoc/HBTU chemistry (31). It has been shown that the structure and composition of the chelating moiety and the spacer group linking the chelator to the peptide play a vital role in determining the physiochemical and pharmacokinetic characteristics of the resultant bioconjugate (39). A well-established renal imaging agent, MAG_3, was used as a chelator, and a hydrophilic aspartic acid residue was used as a spacer, in an effort to enhance urinary excretion and minimize hepatobiliary elimination. MAG_3 is introduced at the *N*-terminus by manual synthesis. The identity and purity of each peptide was confirmed by mass spectrometry and HPLC. It was found that the experimentally determined molecular weights correlated well with the theoretically calculated values (Table I). The synthetic yields were determined to be 20-30% by RP-HPLC analysis.

Radiolabeling with ^{99m}Tc. Radiolabeling of peptides with ^{99m}Tc was achieved by the standard ligand exchange method using sodium potassium tartrate as a weak complexing agent. The radio-HPLC profiles of all radiopeptides showed the formation of one main radioactive compound with some minor peaks. An example of radiolabeling MAG_3-EPPT-MUC1 with ^{99m}Tc is presented in Figure 1. By the exchange labeling approach, the radiolabeling efficiency of ^{99m}Tc-labeled peptides ranged between 65 and 98% (Table II), with a specific radioactivity of greater than 100 Ci/mmol. Usually, the amounts of ^{99m}Tc-peptides produced were below the UV-detection limit during HPLC analysis, which somewhat impeded the exact estimation of the specific radioactivity of the respective radioligands. The extent of ^{99m}Tc-complexation and the radiolabeling yield were found to be pH dependent and the optimal radiolabeling of all the peptides was achieved in the presence of 0.5 M citrate-phosphate buffer pH 10 or higher. This is expected because an alkaline pH facilitates the deprotonation of amide-nitrogens in MAG_3 and the removal of the thiol-protecting group. Both these effects are known to enhance complexation of MAG_3 with ^{99m}Tc (24). The stability of the ^{99m}Tc-conjugates was determined by HPLC at different time intervals. The radiopeptides remained stable (up to 70%) at room temperature for up to 18 h. The HPLC retention times, ranging from 12 to 19.3 min, reflected the expected lipophilicity of the ^{99m}Tc-complexes. ^{99m}Tc-MAG_3-EPPT, the smallest peptide studied, displayed the shortest retention time (12.0 min), hence the lowest lipophilicity (log P=–3.15±0.05) (Table II), whereas ^{99m}Tc-MAG_3-HER2/neu, with the highest retention time of 19.3 min, showed the highest lipophilicity (log P=1.31±0.11) among the tested compounds.

Table II. *Characterization of the radiolabeled peptides.*

Complex	Labeling efficiency (%)	Radio-HPLC t_R (min)	Log P (octanol/saline)
^{99m}Tc-MAG_3-HER2/neu	65	19.3	1.31±0.11
^{99m}Tc-MAG_3-MUC1	75	12.4	–2.53±0.18
^{99m}Tc-MAG_3-HER2/neu-MUC1	90	18.5	–0.40±0.10
^{99m}Tc-MAG_3-EPPT	85	12.0	–3.15±0.05
^{99m}Tc-MAG_3-EPPT-MUC1	98	13.0	–2.50±0.04

Cysteine and histidine challenge. All radiopeptides were challenged with excess cysteine and histidine in order to determine their stability against ligand exchange and/or decomposition. A known amount of each peptide was incubated with excess of cysteine or histidine and the samples were analyzed by HPLC at 1 and 4 h. The results are summarized in Table III. A significant reoxidation (up to 30%) of the ^{99m}Tc-complexes to $^{99m}TcO_4^-$ was detected

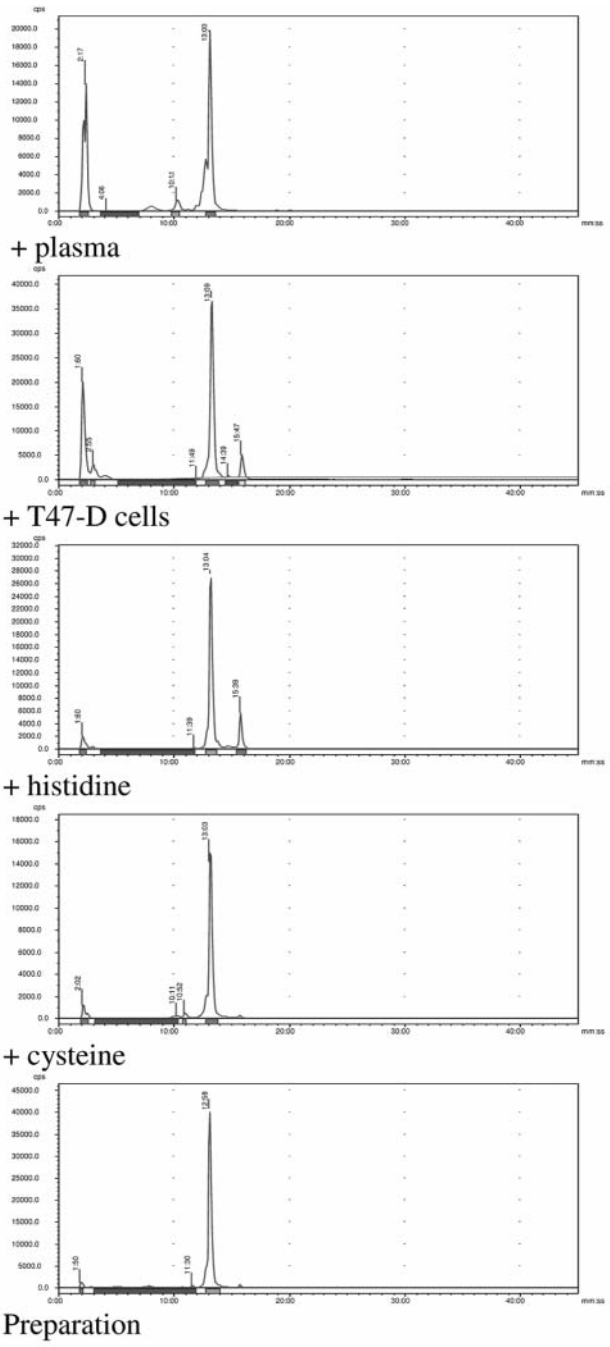

Figure 1. *Representative radio-HPLC chromatograms of ^{99m}Tc-MAG$_3$-EPPT-MUC1 after 1 h incubation with cysteine, histidine, T47-D cells and human plasma at 37˚C.*

even after 1 h at 37˚C, indicating a somewhat weak bond strength of the ^{99m}Tc-complexes. In contrast, these complexes were less efficiently displaced and displayed a relatively higher stability in the presence of excess histidine, suggesting a trend of coordinating ability of different amino acids towards the ^{99m}Tc-MAG$_3$ chelating system. The percentage of ^{99m}Tc-peptides remaining intact after incubation with excess histidine ranged from 90 to 97% at 1 h and 88 to 94% at 4 h, *versus* 70 to 95% at 1 h and 30 to 75% at 4 h with cysteine, clearly demonstrating a high resistance ability of these peptides to histidine displacement and more susceptibility to cysteine transchelation.

Table III. *In vitro stability of different radiopeptides against ligand exchange in excess of cysteine and histidine.*

Complex	% Radioconjugate intact			
	Cysteine		Histidine	
	1 h	4 h	1 h	4 h
^{99m}Tc-MAG$_3$-HER2/neu	70	30	90	88
^{99m}Tc-MAG$_3$-MUC1	94	50	97	94
^{99m}Tc-MAG$_3$-HER2/neu-MUC1	90	40	95	90
^{99m}Tc-MAG$_3$-EPPT	85	60	91	89
^{99m}Tc-MAG$_3$-EPPT-MUC1	95	75	90	88

Lipophilicity. The lipophilic characteristics of the five compounds investigated are listed in Table II. The lipophilicity was determined by measuring the distribution of ^{99m}Tc-peptides between *n*-octanol and saline solutions. A good correlation was observed between the log P values and the HPLC retention times of the radiopeptides under investigation. The results demonstrated that the ^{99m}Tc-MAG$_3$-HER2/neu, which displayed the highest retention time (19.3 min) on HPLC, is the most lipophilic compound (log P=1.31±0.11) evaluated in this study, whereas ^{99m}Tc-MAG$_3$-EPPT, with a retention time of 12.0 min, is the most hydrophilic compound (log P=–3.15±0.05). The obtained log P values varied between 1.31±0.11 and –3.15±0.05 (Table II), revealing a variable degree of lipophilicity of the ^{99m}Tc-complexes evaluated in this study. The lipophilic characteristic of a radiopeptide is important in predicting its route of excretion since hydrophilic radiopharmaceuticals are generally excreted through the renal-urinary pathway, the preferred route of excretion of an effective tumor-imaging peptide radiopharmaceutical.

In vitro stability in plasma and in T47-D cells. The proteolytic degradation of ^{99m}Tc-peptides was determined *in vitro* in human plasma and also in T47-D cells. Following incubation of the radiolabeled peptides in plasma, the plasma proteins were precipitated with acetonitrile/ethanol, and the samples were analyzed by HPLC (Figure 1). All radiopeptides displayed a significant reformation to free $^{99m}TcO_4^-$ (>25%) during incubation in plasma, particularly after 4 h at 37˚C. The metabolic stability varied between 40 and 90% at 1 h, and 30

Table IV. *In vitro stability of ^{99m}Tc-labeled peptides in human plasma and in T47-D cells.*

Complex	% Radioconjugate intact		
	Plasma		T47-D cells
	1 h	4 h	1 h
^{99m}Tc-MAG$_3$-HER2/neu	90	87	80
^{99m}Tc-MAG$_3$-MUC1	80	65	91
^{99m}Tc-MAG$_3$-HER2/neu-MUC1	90	85	95
^{99m}Tc-MAG$_3$-EPPT	40	30	98
^{99m}Tc-MAG$_3$-EPPT-MUC1	55	35	83

Data represent the amount of intact radiopeptides found in plasma and in T47-D cells after incubation at 37˚C.

Table V. *In vitro binding characteristics of ^{99m}Tc-labeled peptides to MCF-7, MDA-MB-231 and T47-D human breast cancer cell lines (mean values±SD).*

Complex	K_d (nM)		
	MCF-7	MDA-MB-231	T47-D
^{99m}Tc-MAG$_3$-HER2/neu	7.92±1.09	3.33±0.92	7.83±1.64
^{99m}Tc-MAG$_3$-MUC1	14.85±1.83	38.77±3.13	7.47±1.53
^{99m}Tc-MAG$_3$-HER2/neu-MUC1	6.75±1.05	11.29±2.03	8.84±1.45
^{99m}Tc-MAG$_3$-EPPT	3.95±0.80	1.55±0.50	12.41±2.09
^{99m}Tc-MAG$_3$-EPPT-MUC1	3.36±1.01	7.79±2.11	25.36±2.99

and 87% at 4 h, revealing a fast degradation of radiopeptides by plasma proteases (Table IV). Enzymatic degradation was even quicker with antitumor-antibody-derived peptides, as only 40 and 55% of ^{99m}Tc-MAG$_3$-EPPT and ^{99m}Tc-MAG$_3$-EPPT-MUC1, respectively, remained intact after 1 h at 37˚C. After 4 h these two peptides were almost completely degraded (~70%). Surprisingly, both these metabolically-unstable peptides have shown a high chemical stability against cysteine and histidine challenge for up to 4 h at 37˚C (Table III).

^{99m}Tc-peptides exhibited a much slower degradation in T47-D cells than in human plasma, as revealed by the HPLC analysis after 1 h incubation with the cells (Table IV). The radiopeptides were found to be relatively stable (≥80%) in the cell culture, an important characteristic, since radioligand stability in the cell culture may be desirable for efficient receptor binding.

In vitro cell binding and internalization. The radiopeptides were evaluated for their tumor targeting properties *in vitro* using three well-characterized human breast cancer cell lines: estrogen receptor-positive MCF-7, estrogen-independent MDA-MB-231, and T47-D human ductal breast cancer (40). These cell lines presented diverse levels of expression of both HER2/neu and MUC1 (12, 41-45). The binding of peptides to their respective receptor-expressing cell lines was determined by saturation assays (Table V). The data demonstrate that ^{99m}Tc-MAG$_3$-HER2/neu showed a similar binding affinity to MCF-7 (7.92±1.09 nM) and T47-D (7.83±1.64 nM) – both these cell lines express moderate levels of HER2/neu (42). Astonishingly, this radiopeptide exhibited a 2-fold higher affinity (3.33±0.92 nM) to MDA-MB-231, despite the fact that this cell line does not have high levels of HER2/neu expression (42, 43). ^{99m}Tc-MAG$_3$-MUC1, on the other hand, displayed a high affinity (7.47±1.53 nM) to receptor-positive T47-D (44, 45), but showed a 2-fold lower affinity (14.85±1.83 nM) to the moderate level expressing MCF-7 (44). The radiopeptide displayed a relatively low affinity (38.77±3.13 nM), to a cell line (MDA-MB-231) with low levels of expression for MUC1 (44, 45). The hybrid-tumor-specific peptides were synthesized with the aim of enhancing the binding efficacy by targeting multiple receptor types, but no significant improvement in terms of binding efficiency over their corresponding nonhybrid derivatives was observed. As can be seen from the data (Table V), ^{99m}Tc-MAG$_3$-HER2/neu-MUC1 displayed a variable affinity profile as compared to its corresponding nonhybrid derivatives (^{99m}Tc-MAG$_3$-HER2/neu and ^{99m}Tc-MAG$_3$-MUC1). The antitumor-antibody-derived peptides (^{99m}Tc-MAG$_3$-EPPT and ^{99m}Tc-MAG$_3$-EPPT-MUC1) showed similar binding to the MCF-7 cell line, 3.95±0.80 nM *vs*. 3.36±1.01 nM, respectively, whereas when binding with T47-D and MDA-MB-231, ^{99m}Tc-MAG$_3$-EPPT was found to be superior as it displayed a 2- to 5-fold higher affinity when compared with its MUC1-hybrid-derivative. The results obtained from *in vitro* binding studies confirmed the significant affinity and specificity of the radiopeptides towards their respective receptor-expressing tumor cell lines.

Table VI. *Internalization of different ^{99m}Tc-labeled peptides into MCF-7, MDA-MB-231 and T47-D cancer cell lines (mean values±SD).*

Complex	% Internalization		
	MCF-7	MDA-MB-231	T47-D
^{99m}Tc-MAG$_3$-HER2/neu	9.0±1.29	33.0±5.35	43.0±2.90
^{99m}Tc-MAG$_3$-MUC1	12.0±3.50	4.0±0.99	30.0±2.50
^{99m}Tc-MAG$_3$-HER2/neu-MUC1	36.0±5.09	32.0±6.54	25.0±2.90
^{99m}Tc-MAG$_3$-EPPT	17.0±3.65	26.0±4.85	20.0±3.14
^{99m}Tc-MAG$_3$-EPPT-MUC1	25.0±3.92	35.0±5.0	20.0±3.69

It is important for peptidic radionuclide therapy that the peptides be internalized into tumor cells after binding to cell-surface receptors (34, 36). *In vitro* internalization studies

Table VII. *In vivo biodistribution of ^{99m}Tc-labeled peptides in Balb/c mice at 1 h and 4 h post-injection (n=3).*

		Blood	Lungs	Stomach	Liver	Intestines[c]	Kidneys	Urine + bladder[a]	Intestines + contents[b]
^{99m}Tc-MAG$_3$-HER2/neu	1 h	1.70±0.17	1.30±0.22	1.17±0.25	3.0±0.82	4.81±1.62	2.65±0.47	25.0±8.31	19.67±3.48
	4 h	1.0±0.13	1.03±0.40	1.41±0.41	1.58±0.36	0.94±0.33	1.70±0.36	40.0±12.48	17.33±3.88
^{99m}Tc-MAG$_3$-MUC1	1 h	0.38±0.06	0.44±0.07	0.35±0.14	1.25±0.39	13.33±4.60	3.68±1.27	60.0±16.13	15.03±5.10
	4 h	0.04±0.01	0.10±0.02	0.63±0.27	0.75±0.15	6.56±1.38	0.86±0.15	40.0±14.41	12.90±2.41
^{99m}Tc-MAG$_3$-HER2/neu-MUC1	1 h	2.03±0.49	0.85±0.09	0.71±0.25	5.83±0.78	5.13±1.68	3.82±0.59	20.0±8.43	20.49±4.31
	4 h	0.91±0.40	0.13±0.03	3.30±0.66	4.14±1.71	1.80±0.45	1.35±0.27	39.0±10.26	20.0±4.82
^{99m}Tc-MAG$_3$- EPPT	1 h	0.22±0.03	0.24±0.04	3.13±1.27	0.33±0.04	4.73±1.98	1.02±0.28	39.0±12.75	15.33±3.85
	4 h	0.18±0.04	0.14±0.02	1.70±0.68	0.29±0.05	2.14±1.00	0.72±0.15	43.0±13.90	10.67±1.90
^{99m}Tc-MAG$_3$- EPPT-MUC1	1 h	0.76±0.19	0.77±0.20	1.62±0.70	0.99±0.32	2.89±1.35	2.01±0.42	68.0±17.13	4.13±1.57
	4 h	0.62±0.14	0.63±0.15	4.0±1.29	0.54±0.10	2.76±1.18	1.83±0.38	67.0±15.51	3.55±0.51

Data are expressed as % injected dose per gram of tissue (mean values±SD). [a,b]The radioactivity in the urine + bladder and intestines + contents are expressed as % injected dose (mean values±SD). [c]Intestines were measured without their contents.

Table VIII. *In vivo biodistribution and tumor uptake studies of the ^{99m}Tc-labeled peptides in nude mice bearing MDA-MB-231 xenografts at 1 and 4 h post-injection (n=3).*

		Blood	Lungs	Stomach	Liver	Intestines[a]	Kidneys	Muscle	Tumor
^{99m}Tc-MAG$_3$-HER2/neu	1 h	1.56±0.69	1.40±0.48	4.13±1.10	4.15±1.02	1.89±0.53	1.90±0.45	0.08±0.02	1.60±0.61
	4 h	1.01±0.41	1.13±0.43	3.37±1.03	3.19±1.01	1.58±0.40	1.51±0.55	0.07±0.01	1.03±0.50
^{99m}Tc-MAG$_3$-MUC1	1 h	0.30±0.09	0.34±0.10	0.99±0.21	2.90±0.89	1.53±0.45	4.87±1.15	0.06±0.01	1.27±0.60
	4 h	0.09±0.02	0.10±0.02	0.40±0.20	0.98±0.15	1.28±0.53	1.48±0.42	0.03±0.00	0.36±0.11
^{99m}Tc-MAG$_3$- EPPT	1 h	0.75±0.21	1.09±0.44	3.90±1.37	1.95±0.93	5.99±1.65	3.52±1.03	0.10±0.02	1.65±0.64
	4 h	0.30±0.09	0.24±0.10	1.10±0.49	1.12±0.55	0.40±0.10	2.12±0.94	0.10±0.02	1.59±0.60
^{99m}Tc-MAG$_3$- EPPT-MUC1	1 h	1.0±0.49	2.0±0.90	2.40±0.97	1.71±0.62	0.82±0.37	4.95±1.27	0.09±0.02	2.20±0.98
	4 h	0.09±0.02	0.10±0.02	0.12±0.03	0.20±0.05	0.25±0.08	1.26±0.34	0.03±0.01	0.63±0.21

Data are expressed as % injected dose per gram of tissue (mean values±SD). [a]Intestines were measured without their contents.

were performed to determine the extent of internalization of the ^{99m}Tc-peptides in human breast cancer cells. In order to differentiate between the tightly cell surface-bound and internalized radioligands, cell-bound radioactivity was treated with acid buffer for 20 min at the end of the binding experiments (46). A rapid and significant internalization was observed for ^{99m}Tc-MAG$_3$-HER2/neu and ^{99m}Tc-MAG$_3$-MUC1, with 43.0±2.90% and 30.0±2.50% , respectively, of the cell surface-bound radiopeptides internalized into T47-D cells after incubation in acid buffer for 20 min at 37˚C. The percent of specific cell surface-bound ^{99m}Tc-peptides internalized into MCF-7 cells varied from 9 to 36% and from 4 to 35% into MDA-MB-231 cells. For T47-D cells, the percent internalized was found to be between 20 and 43% (Table VI). A low internalization (9.0±1.29%) of ^{99m}Tc-MAG$_3$-HER2/neu into MCF-7 cells is most likely because of the low levels of HER2/neu expression by MCF-7 cells (12). ^{99m}Tc-MAG$_3$-MUC1 showed a fairly low intracellular radioactivity (4.0±0.99%) into MDA-MB-231, which may be associated with a very low MUC1 expression on MDA-MB-231 cells (44, 45). These findings of cell-binding and internalization into tumor cells demonstrate that, despite the modifications in the sequences for labeling and the introduction of a spacer group, these peptides maintained their integrity and held sufficient affinity and specificity towards receptor-positive breast cancer cell lines.

In vivo biodistribution and tumor uptake. Table VII summarizes results of biodistribution studies in normal Balb/c mice at 1 and 4 h *p.i*. *In vivo* biodistribution of ^{99m}Tc-peptides were performed first in normal mice (without tumors) to determine normal tissue distribution and clearance kinetics. The results demonstrate that all the conjugates revealed a rapid and efficient clearance from the blood at 1 and 4 h *p.i*. The amount of radioactivity generally retained in the liver ranged from 0.33±0.04% ID/g to 5.83±0.78% ID/g at 1 h, and from 0.29±0.05% ID/g to 4.14±1.71% ID/g at 4 h *p.i*. The highest uptake was by ^{99m}Tc-MAG$_3$-

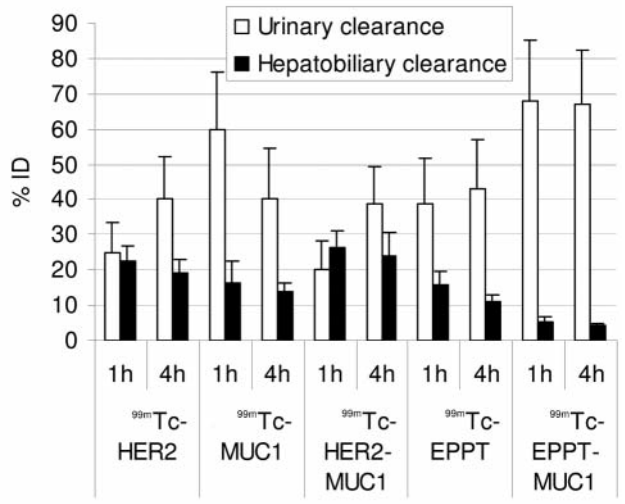

Figure 2. *Clearance of the ^{99m}Tc-labeled peptides from the renal-urinary and hepatobiliary pathways in Balb/c mice at 1 and 4 h post-injection (% ID).*

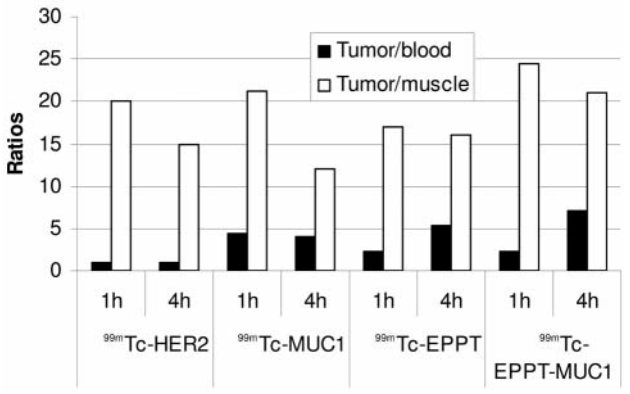

Figure 3. *Tumor-to-blood and tumor-to-muscle ratios for the radiolabeled peptides in nude mice with MDA-MB-231 xenografts at 1 and 4 h p.i.*

HER2/neu-MUC1 (5.83±0.78% ID/g and 4.14±1.71% ID/g, at 1 and 4 h, respectively) possibly in accordance with its high lipophilicity. Although the radioactivity in the intestines was measured without the contents, still a considerably high uptake was observed (up to 13.33±4.60% ID/g). The uptake in the intestines of different complexes varied between 2.89±1.35% ID/g and 13.33±4.60% ID/g at 1 h *p.i.* and between 0.94±0.33% ID/g and 6.56±1.38% ID/g at 4 h *p.i.* The accumulation in the kidneys ranged from 1.02±0.28% ID/g to 3.68±1.27% ID/g at 1 h *p.i.* and from 0.72±0.15% ID/g to 1.83±0.38% ID/g at 4 h *p.i.*, demonstrating a low uptake/retention of these complexes by the kidneys. The radioactivity accumulation in the stomach for all the peptides (except for ^{99m}Tc-MAG$_3$-EPPT) increased over time, with a maximum uptake of 4.0±1.29% ID/g at 4 h *p.i.*, showing *in vivo* stability of the ^{99m}Tc-complexes and insignificant reformation to $^{99m}TcO_4^-$. The radiopeptide ^{99m}Tc-MAG$_3$-EPPT-MUC1, with the highest stomach uptake (4.0±1.29% ID/g, 4 h), also showed a relatively poor stability in human plasma *in vitro*, signifying a correlation between *in vitro* and *in vivo* stability but not with the overall biodistribution and clearance pattern. The uptake in the lungs was also low (values varied from 0.10±0.02% ID/g to 1.30±0.22% ID/g) both at 1 and 4 h *p.i.* The data suggest that the introduction of a hydrophilic spacer (aspartic acid) only minimally improved renal excretion of the various bioconjugates studied. In general, a rapid and efficient clearance of radioactivity was achieved from all the organs except the intestines, highlighting the favorable biodistribution profiles of these compounds.

It is worth mentioning that precautions were taken to maximize collection of urine, but because of the practical difficulties, complete collection of urine from mice after sacrifice is not always possible, which may result in underestimation of urinary excretion. It can be assumed that the majority of the radioactivity in the intestines arrives *via* the hepatobiliary system. It was observed that most of the radioactivity was found in the contents of the intestines. The clearance properties of ^{99m}Tc-complexes are presented in Figure 2. It is apparent from the clearance patterns in normal mice that the radiopeptides cleared by both the hepatobiliary and renal-urinary pathway, but the degree of clearance from each route varies from peptide to peptide. For instance, ^{99m}Tc-MAG$_3$-HER2/neu, the most lipophilic complex studied, with a log P=1.31±0.11, was cleared significantly by both the renal-urinary and the hepatobiliary systems. The clearance pattern of ^{99m}Tc-MAG$_3$-HER2/neu-MUC1 was nearly identical to that of the analogous ^{99m}Tc-MAG$_3$-HER2/neu. In contrast, ^{99m}Tc-MAG$_3$-MUC1 was excreted mainly through the renal-urinary route with some elimination *via* the hepatobiliary system. The most favorable clearance pattern was observed for ^{99m}Tc-MAG$_3$-EPPT-MUC1, with the renal-urinary pathway as the main excretory route (67-68% ID) in accordance with the hydrophilic characteristic (log P=–2.50±0.04) of this radioconjugate. The corresponding ^{99m}Tc-MAG$_3$-EPPT also behaved similarly, but the extent of renal-urinary excretion was found to be slightly lower (39-43% ID) than that of ^{99m}Tc-MAG$_3$-EPPT-MUC1. The clearance studies underline the importance of the degree of lipophilicity as one of the determining factors in the clearance passage of a radiopharmaceutical.

^{99m}Tc-MAG$_3$-HER2/neu, ^{99m}Tc-MAG$_3$-MUC1, ^{99m}Tc-MAG$_3$-EPPT and ^{99m}Tc-MAG$_3$-EPPT-MUC1 were further evaluated in nude mice bearing MDA-MB-231 xenografts to determine their ability to target human breast cancer *in vivo*

(Table VIII). The highest tumor uptake was achieved with the analog ^{99m}Tc-MAG$_3$-EPPT-MUC1, 2.20±0.98% ID/g, as early as 1 h *p.i.*, which fell to 0.63±0.21% ID/g at 4 h *p.i.* Interestingly, the same compound exhibited the most favorable clearance kinetics in normal mice (Table VII). However, an enhanced uptake of this compound in most of the major organs, especially in the kidneys (4.95±1.27% ID/g, 1h), was found in tumor-bearing mice as compared to normal mice. A blocking dose of MAG$_3$-EPPT decreased the uptake of ^{99m}Tc-MAG$_3$-EPPT-MUC1 in the tumor, intestines and kidneys, whereas uptake in the lungs was increased (data not shown). In nude mice bearing breast tumor xenografts, the accumulation in the tumor was moderate for all the four conjugates examined particularly at 1 h *p.i.* (Table VIII). The tumor uptake values varied from 1.27±0.60% ID/g to 2.20±0.98% ID/g at 1 h and from 0.36±0.11% ID/g to 1.59±0.60% ID/g at 4 h *p.i.* The radiopeptides showed greater accumulation in the tumors than in the blood and muscle in the MDA-MB-231-bearing nude mice. Though the uptake in tumors was not very high for any of the peptides tested (up to 2.20±0.98% ID/g), slow tumor washout was observed for these peptides and in particular for ^{99m}Tc-MAG$_3$-EPPT (1.65±0.64% ID/g at 1 h *vs.* 1.59±0.60% ID/g at 4 h) and ^{99m}Tc-MAG$_3$-HER2/neu (1.60±0.61% ID/g at 1 h *vs.* 1.03±0.50% ID/g at 4 h). The tumor retention of the two other peptides (^{99m}Tc-MAG$_3$-EPPT-MUC1 and ^{99m}Tc-MAG$_3$-MUC1) was found to be relatively low (with 71-72% washout).

Radioactivity uptake pattern for most tissues was comparable in nude and normal mice, but in some cases organ uptake was lower in tumor-bearing mice than in normal mice, especially in the intestines. The uptake in the kidneys was low to moderate and ranged between 1.26±0.34% ID/g and 4.95±1.27% ID/g at both time points. Less than 6% ID/g of uptake was obtained for the major organs examined in tumor-bearing mice (Table VIII).

Tumor-to-nontumor ratios were also calculated and are presented in Figure 3. For ^{99m}Tc-MAG$_3$-EPPT-MUC1, the tumor-to-blood ratios was approximately 2:1 at 1 h *p.i.* and 7:1 at 4 h *p.i.* The relatively low tumor-to-blood ratio at 1 h *p.i.* is due to the presence of a somewhat high radioactivity in the blood. The tumor-to-muscle ratios of this peptide were approximately 25:1 at 1 h *p.i.* and 21:1 at 4 h *p.i.* The other peptides (^{99m}Tc-MAG$_3$-HER2/neu, ^{99m}Tc-MAG$_3$-MUC1 and ^{99m}Tc-MAG$_3$-EPPT) also displayed fairly good tumor-to-blood ratios varying from 1:1 to 4:1 at 1 h *p.i.* and from 1:1 to 5:1 at 4 h *p.i.* The tumor-to-muscle ratios ranged from 17:1 to 21:1 at 1 h *p.i.* and from 12:1 to 16:1 at 4 h *p.i.*, demonstrating the possible potential of these peptides for targeting breast tumors *in vivo*. A trend of increased tumor-to-blood ratios and reduction in tumor-to-muscle ratios over time was obtained for these peptides. These results suggest that the peptides evaluated in this study indeed have favorable characteristics which may make them potential candidates for imaging breast cancer *in vivo*.

The preparation, and *in vitro* and *in vivo* evaluation of five new peptides derived from tumor-specific antigens and antitumor-antibody were investigated in this study. The peptides, after radiolabeling with ^{99m}Tc *via* ligand exchange, displayed good chemical and metabolic stability *in vitro*. The data from *in vitro* binding studies performed with human breast cancer cell lines presenting diverse levels of receptor expression confirmed the significant affinity, in a low nanomolar range, towards the respective receptor-expressing cell lines. Moreover, the peptides displayed a good degree of internalization into the cells after binding to the cell surface receptors. *In vivo* biodistribution in Balb/c mice was characterized by an efficient clearance from the blood and a low to moderate uptake/retention of radiopeptides by the major organs (up to 6% ID/g), with the exception of the intestines, which retained up to 13% ID/g. These peptides, with variable degrees of lipophilicity, exhibited different clearance profiles. The hydrophilic peptides, such as ^{99m}Tc-MAG$_3$-EPPT-MUC1 and ^{99m}Tc-MAG$_3$-MUC1, cleared mainly through the renal-urinary route while the peptide with a higher lipophilicity, ^{99m}Tc-MAG$_3$-HER2/neu, was eliminated by both the renal-urinary and hepatobiliary system. In nude mice with breast tumor xenografts, moderate uptake in the tumor was observed with favorable tumor-to-blood and tumor-to-muscle ratios, indicating the tumor targeting potential of these peptides. The data suggest that the peptides under investigation have favorable *in vitro* and *in vivo* properties which make them attractive candidates for the detection of breast cancer *in vivo*. Although more studies are required to determine the full potential of these peptides as breast cancer imaging agents, these findings provide useful information for designing and developing new tumor-specific peptides for targeting tumors that overexpress specific receptors for the peptides.

Acknowledgements

The authors would like to thank Marsood Ahmad for help in animal experiments and Dr. H. Ghebeh for the preparation of cells. This work was supported by a grant from the KACST (Grant No. M-S-12-2 awarded to S.M.O.).

References

1 Knutson KL, Schiffman K and Disis ML: Immunization with a HER-2/neu helper peptide vaccine generates HER-2/neu CD8 T-cell immunity in cancer patients. J Clin Invest *107*: 477-484, 2001.

2 Brossart P, Wirths S, Stuhler G, Reichardt VL, Kanz L and Brugger W: Induction of cytotoxic T-lymphocyte responses *in vivo* after vaccinations with peptide-pulsed dendritic cells. Blood *96*: 3102-3108, 2000.

3 Knutson KL, Schiffman K, Cheever MA and Disis ML: Immunization of cancer patients with a HER-2/neu. HLA-A2 peptide, p. 369-377, results in short-lived peptide-specific immunity. Clin Cancer Res *8*: 1014-1018, 2002.

4 Apostolopoulos V, Matsoukas J, Plebanski M and Mavromoustakos T: Applications of peptide mimetics in cancer. Curr Med Chem *9*: 411-420, 2002.

5 Moore A, Medarova Z, Potthast A and Dai G: *In vivo* targeting of underglycosylated MUC-1 tumor antigen using a multimodal imaging probe. Cancer Res *64*: 1821-1827, 2004.

6 Müller S and Hanisch F-G: Recombinant MUC1 probe authentically reflects cell-specific *O*-glycosylation profiles of endogenous breast cancer mucin. J Biol Chem *277*: 26103-26112, 2002.

7 Yang Z, Bagheri-Yarmand R, Balasenthil S, Hortobagyi G, Sahin AA, Barnes CJ and Kumar R: HER2 regulation of peroxisome proliferator-activated receptor γ (PPARγ) expression and sensitivity of breast cancer cells to PPARγ ligand therapy. Clin Cancer Res *9*: 3198-3203, 2003.

8 Press MF, Cordon-Cardo C and Slamon DJ: Expression of the *HER-2/neu* proto-oncogene in normal human adult and fetal tissues. Oncogene *5*: 953-962, 1990.

9 Natali PG, Nicotra MR, Bigotti A, Venturo I, Slamon DJ, Fendly BM and Ullrich A: Expression of the p185 encoded by *her2* oncogene in normal and transformed human tissues. Int J Cancer *45*: 457-461, 1990.

10 Olafsen T, Tan GJ, Cheung C-W, Yazaki PJ, Park JM, Shively JE, Williams LE, Raubitschek AA, Press MF and Wu AM: Characterization of engineered anti-p185HER-2 (scFv-CH3)2 antibody fragments (minibodies) for tumor targeting. Protein Eng Des Sel *17*: 315-323, 2004.

11 Engfeldt T, Orlova A, Tran T, Bruskin A, Widström C, Karlström A E and Tolmachev V: Imaging of HER2-expressing tumours using a synthetic affibody molecule containing the ^{99m}Tc-chelating mercaptoacetyl-glycyl-glycyl-glycyl (MAG_3) sequence. Eur J Nucl Med Mol Imaging *34*: 722-733, 2007.

12 Pero SC, Shukla GS, Armstrong AL, Peterson D, Fuller SP, Godin K, Kingsley-Richards SL, Weaver DL, Bond J and Krag DN: Identification of a small peptide that inhibits the phosphorylation of ErbB2 and proliferation of ErbB2 overexpressing breast cancer cells. Int J Cancer *111*: 951-960, 2004.

13 Behr T M, Béhé M and Wörmann B: Trastuzumab and breast cancer. N Engl J Med *345*: 995-996, 2001.

14 Lub-de Hooge MN, Kosterink J GW, Perik PJ, Nijnuis H, Tran L, Bart, J, Suurmeijer AJH, de Jong S, Jager PL and de Vries E GE: Preclinical characterisation of ^{111}In-DTPA-trastuzumab. Br J Pharmacol *143*: 99-106, 2004.

15 Slamon DJ, Leyland-Jones B, Shak S, Fuchs H, Paton V, Bajamonde A, Fleming T, Eiermann W, Wolter J, Pegram M, Baselga J and Norton L: Use of chemotherapy plus a monoclonal antibody against HER2 for metastatic breast cancer that overexpresses HER2. N Engl J Med *344*: 783-792, 2001.

16 Tolmachev V, Nilsson FY, Widström C, Andersson K, Rosik D, Gedda L, Wennborg A and Orlova A: ^{111}In-Benzyl-DTPA–ZHER2: 342, an affibody-based conjugate for *in vivo* imaging of HER2 expression in malignant tumors. J Nucl Med *47*: 846-853, 2006.

17 De Santes K, Slamon D, Anderson S K, Shepard M, Fendly B, Maneval D and Press D: Radiolabeled antibody targeting of the HER-2/neu oncoprotein. Cancer Res *52*: 1916-1923, 1992.

18 Zalutsky MR, Xu FJ, Yu Y, Foulon CF, Zhao X-G, Slade SK, Affleck DJ and Bast RC Jr: Radioiodinated antibody targeting of the HER-2/neu oncoprotein: Effects of labeling method on cellular processing and tissue distribution. Nucl Med Biol *26*: 781-790, 1999.

19 Tang Y, Wang J, Scollard DA, Mondal H, Holloway C, Kahn HJ and Reilly RM: Imaging of HER2/neu-positive BT-474 human breast cancer xenografts in athymic mice using ^{111}In-trastuzumab (Herceptin™) Fab fragments. Nucl Med Biol *32*: 51-58, 2005.

20 Tsai SW, Sun YY, Williams LE, Raubitschek AA, Wu AM and Shively JE: Biodistribution and radioimmunotherapy of human breast cancer xenografts with radiometal-labeled DOTA conjugated anti-HER2/neu antibody 4D5. Bioconjugate Chem *11*: 327-334, 2000.

21 Britz-Cunningham SH and Adelstein SJ: Molecular targeting with radionuclides: State of science. J Nucl Med *44*: 1945-1961, 2003.

22 Park B-W, Zhang H-T Wu C, Berezov A, Zhang X, Dua R, Wang Q, Kao G, O'Rourke D M, Greene MI and Murali R: Rationally designed anti-HER2/neu peptide mimetic disables P185$^{HER/neu}$ tyrosine kinases *in vitro* and *in vivo*. Nat Biotechnol *18*: 194-198, 2000.

23 Okarvi SM: Peptide-based radiopharmaceuticals and cytotoxic conjugates: Potential tools against cancers. Cancer Treat Rev *34*: 13-26, 2008.

24 Okarvi SM, Adriaens P and Verbruggen A: Comparison of the labelling characteristics of mercaptoacetyltriglycine (MAG_3) with different S-protective groups. J Labelled Cpd Radiopharm *39*: 853-874, 1997.

25 Anderson BW, Peoples GE, Murray JL, Gillogly MA, Gershenson DM and Ioannides CG: Peptide priming of cytolytic activity to HER-2 epitope 369-377 in healthy individuals. Clin Cancer Res *6*: 4192-4200, 2000.

26 Correa I and Plunkett T: Update on HER-2 as a target for cancer therapy. HER2/neu peptides as tumour vaccines for T-cell recognition. Breast Cancer Res *3*: 399-403, 2001.

27 Zaks TZ and Rosenberg SA: Immunization with a peptide epitope (p. 369-377) from HER-2/neu leads to peptide-specific cytotoxic T lymphocytes that fail to recognize HER-2/neu$^+$ tumors. Cancer Res *58*: 4902-4908, 1998.

28 Agrawal B, Reddish MA, Christian B, VanHeele A, Tang L, Koganty RR and Longenecker BM: The anti-MUC1 monoclonal antibody BCP8 can be used to isolate and identify putative major histocompatibility complex class 1 associated amino acid sequences. Cancer Res *58*: 5151-5156, 1998.

29 Okarvi SM: Synthesis, radiolabeling and *in vitro* and *in vivo* characterization of a technetium-99m-labeled alpha-M2 peptide as a tumor imaging agent. J Peptide Res *63*: 460-468, 2004.

30 Sivolapenko GB, Douli V, Pectasides D, Skarlos D, Sirmalis G, Hussain R, Cook J, Courtenay-Luck NS, Merkouri E, Konstantinides K and Epenetos AA: Breast cancer imaging with radiolabelled peptide from complementarity-determining region of antitumour antibody. Lancet *346*: 1662-1666, 1995.

31 Grant GA: Synthetic Peptides. New York, Oxford University Press, 2002.

32 Brandau W, Bubeck B, Eisenhut M and Taylor DM: Technetium-99m labeled renal function and imaging agents: III. Synthesis of ^{99m}Tc-MAG_3 and biodistribution of by-products. Appl Radiat Isot *39*: 121-129, 1988.

33 Fukuoka M, Kiyohara T, Kobayashi T, Kojima A, Tanaka A and Kubodera A: Synthesis and preclinical evaluation of technetium-99m-labeled hippurate analogues. Nucl Med Biol *22*: 181-191, 1995.

34 Okarvi SM and Jammaz IA: Preparation and *in vitro* and *in vivo* evaluation of technetium-99m-labeled folate and methotrexate conjugates as tumor imaging agents. Cancer Biother Radio *21*: 49-60, 2006.
35 Lundquist P, Wilking H, Höglund AU, Sandell J, Bergström M, Hartvig P and Långström B: Potential of [^{11}C]DASB for measuring endogenous serotonin with PET: binding studies. Nucl Med Biol *32*: 129-136, 2005.
36 Breeman W A, de Jong M, Erion J L, Bugaj J E, Srinivasan A, Bernard B F, Kwekkeboom D J, Visser T J and Krenning E P: Preclinical comparison of ^{111}In-labeled DTPA- or DOTA-bombesin analogs for receptor targeted scintigraphy and radionuclide therapy. J Nucl Med *43*: 1650-1656, 2002.
37 Mandler R, Wu C, Sausville EA, Roettinger AJ, Newman DJ, Ho DK, King CR, Yang D, Lippman ME, Landolfi NF, Dadachova E, Brechbiel MW and Waldmann TA: Immuno-conjugates of geldanamycin and anti-HER2 monoclonal antibodies: Antiproliferative activity on human breast carcinoma cell lines. J Natl Cancer Inst *92*: 1573-1581, 2000.
38 Guide for the Care and Use of Laboratory Animals. Washington, D.C., National Academy Press: 1996.
39 Decristoforo C and Mather SJ: The influence of chelator on the pharmacokinetics of ^{99m}Tc-labelled peptides. Q J Nucl Med *46*: 195-205, 2002.
40 Zajchowski DA, Bartholdi MF, Gong Y, Webster L, Liu H-L, Munishkin A, Beauheim C, Harvey S, Ethier SP and Johnson P H: Identification of gene expression profiles that predict the aggressive behavior of breast cancer cells. Cancer Res *61*: 5168-5178, 2001.
41 Mullin AE and Jean-Claude B: HER2/*neu* oncogene and sensitivity to the DNA-interactive drug Doxorubicin. McGill J Med *4*: 9-15, 1998.
42 Cabioglu N, Summy J, Miller C, Parikh NU, Sahin AA, Tuzlali S, Pumiglia K, Gallick GE and Price JE: CXCL-12/stromal cell-derived factor-1α transactivates HER2-neu in breast cancer cells by a novel pathway involving Src kinase activation. Cancer Res *65*: 6493-6497, 2005.
43 Ueno NT, Yu D and Hung M-C: Chemosensitization of HER-2/*neu*-overexpressing breast cancer cells to paclitaxel (Taxol) by adenovirus type 5 *E1A*. Oncogene *15*: 953-960, 1997.
44 Walsh MD, Luckie SM, Cummings MC, Antalis TM and McGuckin MA: Heterogeneity of MUC1 expression by human breast carcinoma cell lines *in vivo* and *in vitro*. Breast cancer Res Treat *58*: 255-266, 2000.
45 Dwyer RM, Bergert ER, O'Connor MK, Gendler SJ and Morris JC: *In vivo* radionuclide imaging and treatment of breast cancer xenografts after MUC1-driven expression of the sodium iodide symporter. Clin Cancer Res *11*: 1483-1489, 2005.
46 Siegrist W, Solca F, Stutz S, Giuffre L, Carrel S, Girard J and Eberle AN: Characterization of receptors for α-melanocyte-stimulating hormone on human melanoma cells. Cancer Res *49*: 6352-6358, 1989.

Received November 3, 2008
Revised January 7, 2009
Accepted February 13, 2009